

1 **Review of MS. MS No.: EGUSPHERE-2025-6531**

2 **Title:** Estimation of nocturnal boundary layer height in the central Amazon, supported by gas
3 concentration profiles

4
5 Response (blue color) to anonymous **Referee #1** (black). The original manuscript was
6 changed accordingly. Please note that all line numbers indicated in our responses refer to the
7 tracked-changes version of the revised manuscript.

8
9 **General comments**

10
11 This manuscript addresses a timely and potentially interesting topic of the dynamics of the
12 nocturnal boundary layer and the impact on the gas concentration profiles in a remote location
13 of the Amazonia. The meteorological and atmospheric composition data is very
14 comprehensive. However, the analysis and interpretation remain largely descriptive and do
15 not sufficiently engage with the underlying physical mechanisms or relevant observational and
16 theoretical studies. Substantial additional work would be required to strengthen the physical
17 interpretation of the dynamics of the Amazonian Nocturnal Boundary Layer (ANBL) and fully
18 exploit the observations. Given the extent of revisions needed, we recommend rejection at
19 this stage, with the encouragement that the authors resubmit a thoroughly revised manuscript
20 after deeper physical and observational analysis. In the following, we provide several points
21 where the analysis could be further elaborated to establish clearer physical causality.

22
23 We thank Reviewer#1 for their constructive comments. We have carefully revised the
24 manuscript (MS) and incorporated substantial additional analyses addressing the key points
25 raised by the Reviewer. These include a more explicit treatment of the physical mechanisms
26 controlling the nocturnal boundary layer, an extended climatological context, and a clearer
27 quantification of the main drivers of ANBL variability. We believe that these additions
28 significantly improve the robustness of the results and the physical interpretation, and that the
29 actual revised manuscript addresses the concerns raised by the Reviewer. Below, we respond
30 to each comment in detail and describe the corresponding changes implemented in the
31 revised version of the MS. The line numbers referenced here are based on the revised version.

32
33 **Specific comments**

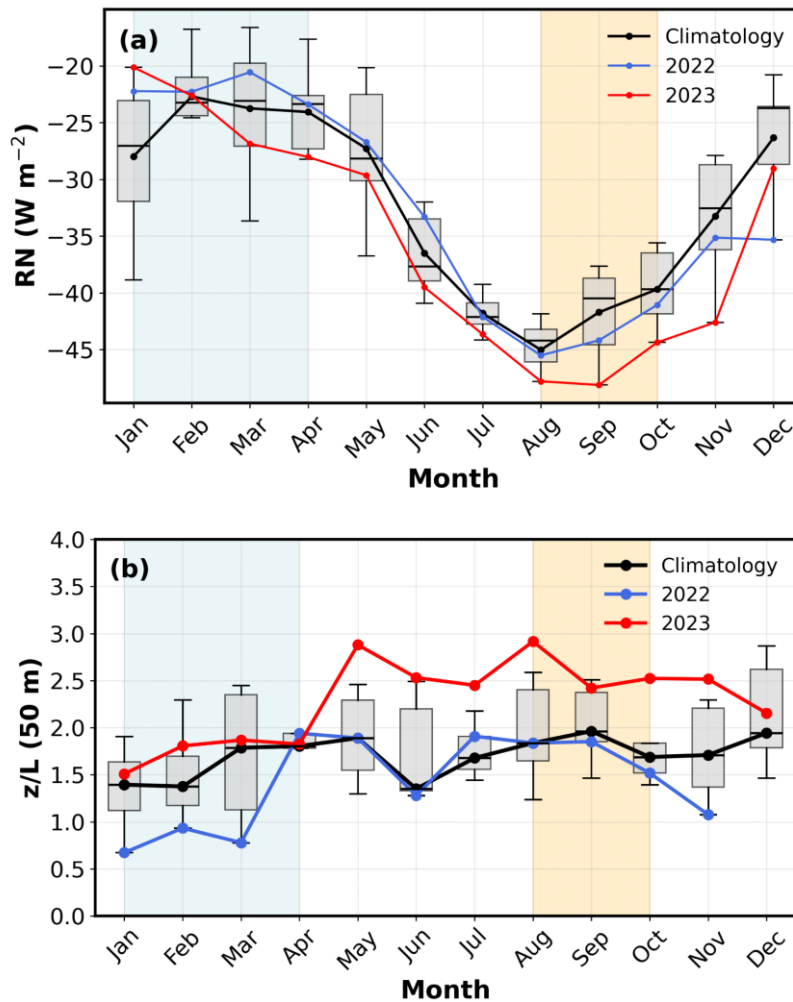
34
35 1. The study could benefit from an extended climatology of the stability of the ANBL. Based
36 on only one La Nina year (2022) and one El Nino year (2023) it is hard to explain which part
37 of the variability can be attributed to the ENSO and which part to the annual variability. With
38 an elaborate description of the yearly variation, the ENSO effect could be clearly quantified.

39
40 We thank the Reviewer for their important comment. We agree that an extended climatology
41 of ANBL stability is necessary to place the 2022 and 2023 results in the context of the
42 background interannual variability. At the same time, we would like to clarify an observational
43 limitation of the dataset. The full vertical profile of sonic anemometers up to 325 m at Amazon
44 Tall Tower Observatory (ATTO) became operational only in August 2021. Therefore, reliable
45 estimates of the nocturnal boundary-layer height (h_n) are only available from 2022 onward.
46 Although 2024 could provide an additional year of h_n estimates, this year was also affected
47 by the aftermath of the 2023 El Niño and cannot be treated as an independent climatological
48 reference (Souza et al., 2024).

49
50 To address this limitation, we added an extended climatological analysis based on variables
51 available over a longer period and directly linked to ANBL variability: nocturnal net radiation
52 (R_n) and the atmospheric stability parameter (z/L). These variables provide important
53 information about nocturnal radiative cooling and the atmospheric stability, both of which
54 strongly influence ANBL behavior. This climatology was calculated for the 2016–2024 period
55 using the same nighttime interval adopted throughout the manuscript (00:00–09:00 UTC).

56 Figure 1 (of this document) shows that the dry season is generally characterized by higher
 57 negative net radiation values, consistent with stronger nocturnal radiative cooling, and by
 58 larger z/L values, indicating more stable conditions. The year 2023 shows z/L values above
 59 the climatological mean during most months, particularly from May onward, whereas 2022
 60 remains generally closer to, or below, the climatological mean during several months. This
 61 additional analysis supports the interpretation that the shallower ANBL observed in 2023 was
 62 associated with enhanced nocturnal stability.

63
 64 We included this discussion in the revised manuscript to place the analyzed years within the
 65 observed ATTO climatology context. Since radiative cooling and stability are relevant controls
 66 on nocturnal turbulence and ANBL structure, these deviations from the climatology can be
 67 associated to the observed differences in h_n between 2022 and 2023.
 68



69
 70 Figure 1 (Figure 3 in new version of the manuscript). Monthly mean of (a) net radiation (Rn)
 71 at 81 m and (b) stability parameter (z/L) at 50 m for the nighttime period (00:00–09:00 UTC).
 72 Grey boxplots represent the monthly climatological distribution for 2016–2024. Shaded blue
 73 and orange areas indicate the wet and dry seasons, respectively .
 74

75 In the new version of the manuscript, it was added:

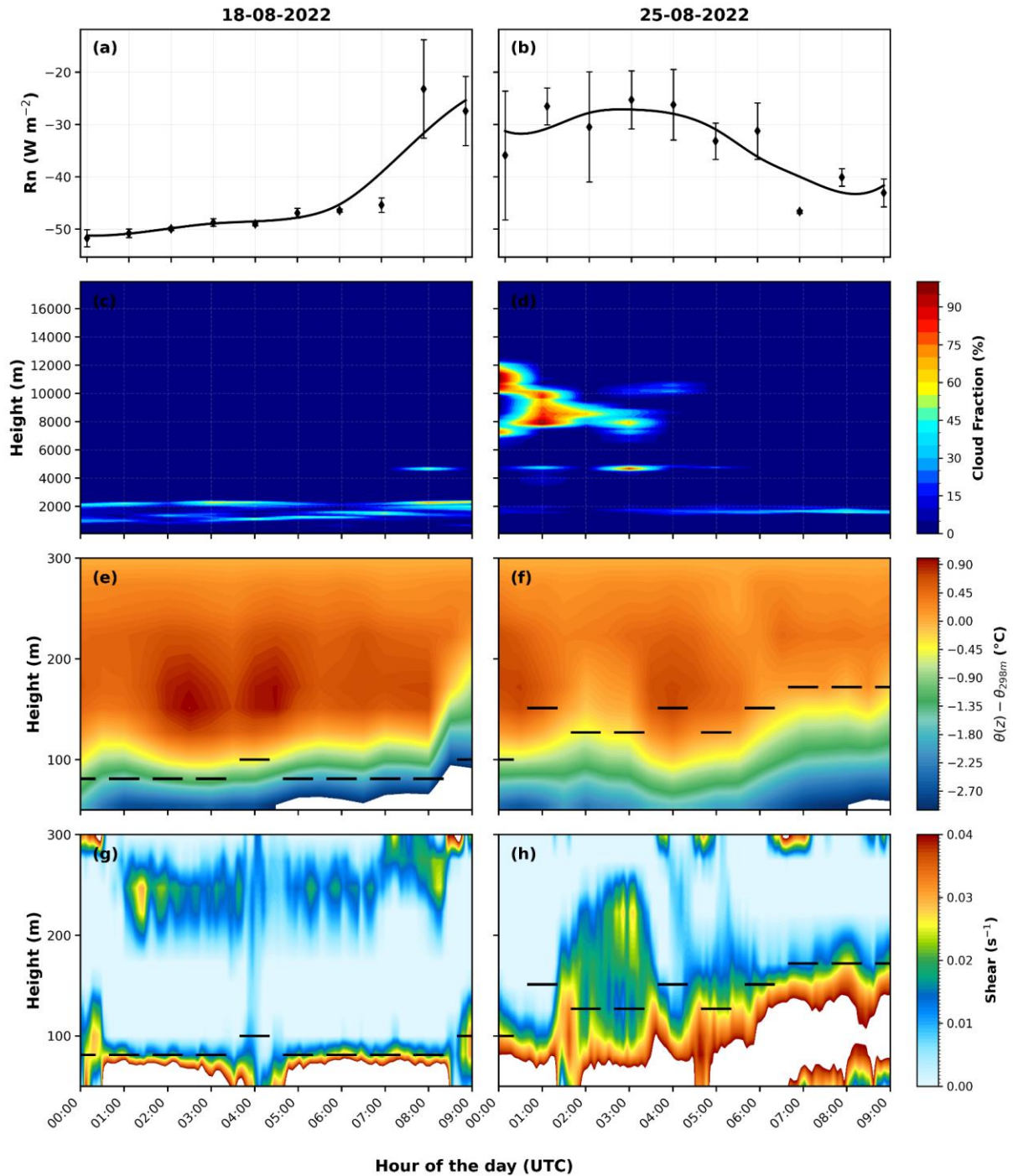
76
 77 L 187- 195: To place the analyzed years in a broader climatological context, Figure 3 shows
 78 the monthly nocturnal climatology of Rn and z/L for the 2016–2024 period, using the same
 79 nighttime interval adopted in this study (00:00–09:00 UTC). The climatology highlights a clear
 80 seasonal cycle, with stronger nocturnal radiative cooling during the dry season associated with

81 higher z/L values and therefore more stable atmospheric conditions. In 2023, z/L values were
82 higher than the climatological mean during most months, especially from May onward,
83 whereas 2022 remained closer to, or below, the climatological mean values. These departures
84 from the ATTO climatology indicate that the two analyzed years experienced distinct nocturnal
85 radiative cooling and stability conditions. Since R_n and z/L are relevant controls on turbulence
86 intensity and the vertical structure of the nocturnal boundary layer, these differences may be
87 related to the contrasting h_n behavior observed in 2022 and 2023 (discussed in section 3.2).
88

89 2. In relation to this a clearer identification and quantification of the main drivers would
90 substantially strengthen the manuscript. For example, Figure 2 of this document presents
91 longwave radiative cooling, but its role in enhancing nocturnal stratification is not sufficiently
92 discussed. Further elaboration on how radiative cooling contributes to the stability of the
93 nocturnal boundary layer would be valuable. Similarly, in lines 200–205, the manuscript
94 discusses shear associated with changes in wind direction, which is a well-known mechanism
95 for turbulence generation. Quantifying the magnitude of this shear using the available
96 observations, and assessing its relative importance in sustaining turbulence and shaping the
97 nocturnal boundary layer structure, would greatly improve the physical interpretation. We think
98 here it can be convenient to connect and relate their findings with recent work of Mahrt and
99 Acevedo (Boundary-layer Meteorology 187:141–161, 2023 and references therein).

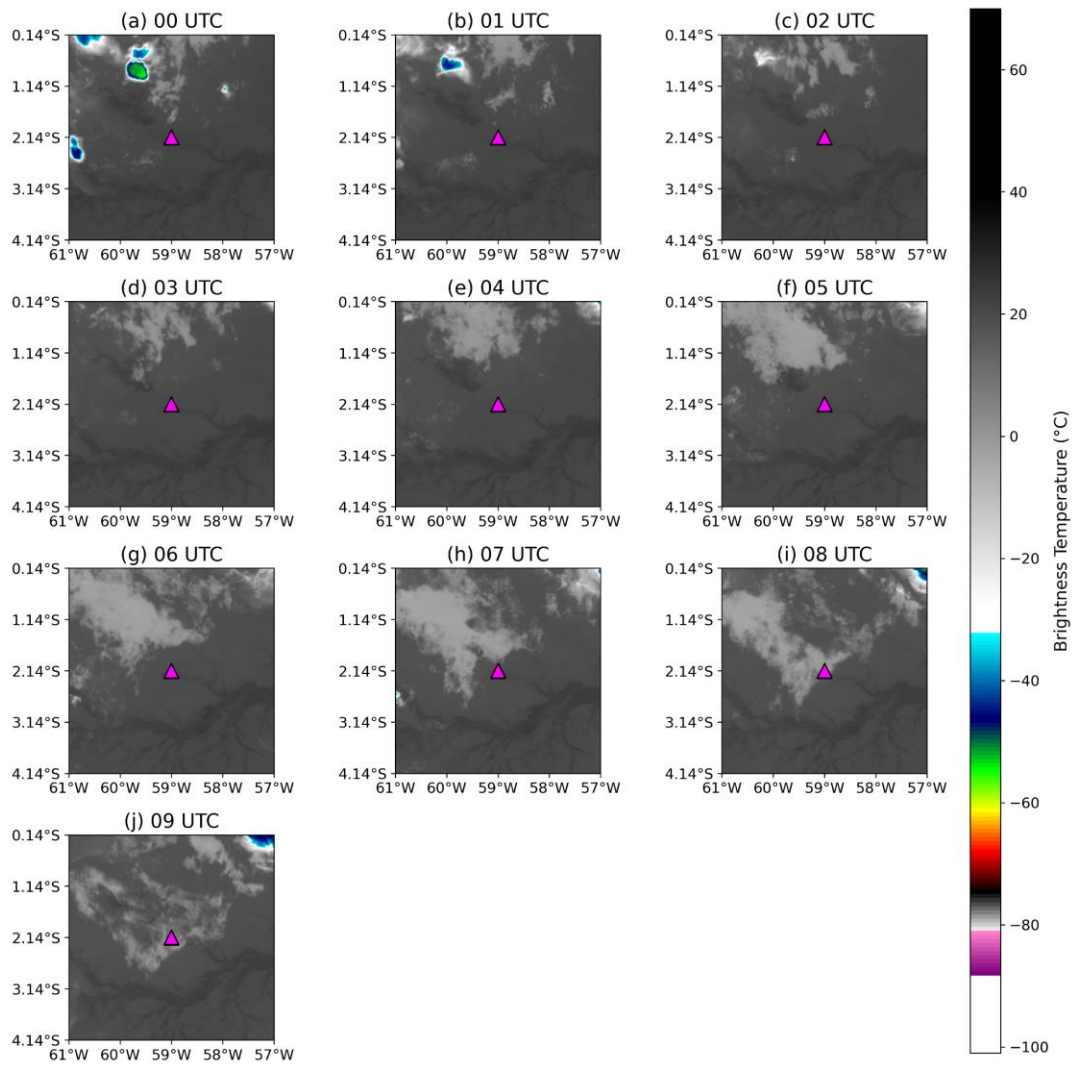
100 We thank Reviewer #1 for this comment. To better quantify the main drivers of NBL evolution,
101 we expanded the analysis of the two case-study nights showed in the previous version of the
102 manuscript, including net radiation (R_n) at 81 m, cloud fraction (%), vertical profile of the
103 potential temperature (θ), and vertical wind shear (dU/dz) for 18 and 25 August 2022 (Figure
104 2 of this document). To compute wind shear, third-order polynomial fits were applied to the
105 wind speed profiles ($U(z)$), from which analytical vertical derivatives were calculated. Cloud
106 cover was estimated from observations obtained by the Cloud Radar Profiler (METEK MIRA-
107 35C) installed at the ATTO site. GOES-16 IR Channel 13 ($10.3\ \mu\text{m}$) brightness temperature
108 imagery was additionally used to illustrate cloud cover conditions during the two nights
109 (Figures 3 and 4 of this document).
110

111 The night of 18 August 2022 represents a strongly stratified and more decoupled case
112 compared to 25 August 2022. Strong radiative cooling (Fig. 2a), reduced cloud occurrence
113 (Fig. 2c and Fig. 3), and a pronounced vertical potential temperature gradient (Fig. 2e), were
114 associated with a shallow h_n , mostly around 80–100 m. Despite the presence of wind shear
115 at some levels, the strong thermal stratification suggests that mechanically generated
116 turbulence aloft was not efficiently coupled downward to the layer near the canopy. This
117 behavior is consistent with a layered nocturnal structure in which the shallow surface-based
118 layer remains isolated from the air above, similar to the regime described by Mahrt and
119 Acevedo (2023). In contrast, the night of 25 August 2022 showed larger cloud cover (Fig. 2d
120 and Fig. 4), reduced radiative cooling during the early night (Fig. 2b), and weaker thermal
121 stratification (Fig. 2f). Wind shear extended to higher levels (Fig. 2h), reaching approximately
122 150–170 m, close to h_N . This suggests that mechanical forcing contributed to sustaining
123 turbulence over a deeper layer under weaker stratification. Therefore, the differences between
124 those two nights are interpreted as the result of the balance between radiative cooling, which
125 enhances thermal stratification and suppresses turbulence, and shear-generated mechanical
126 turbulence, which can deepen or sustain the NBL when coupling is possible.
127
128



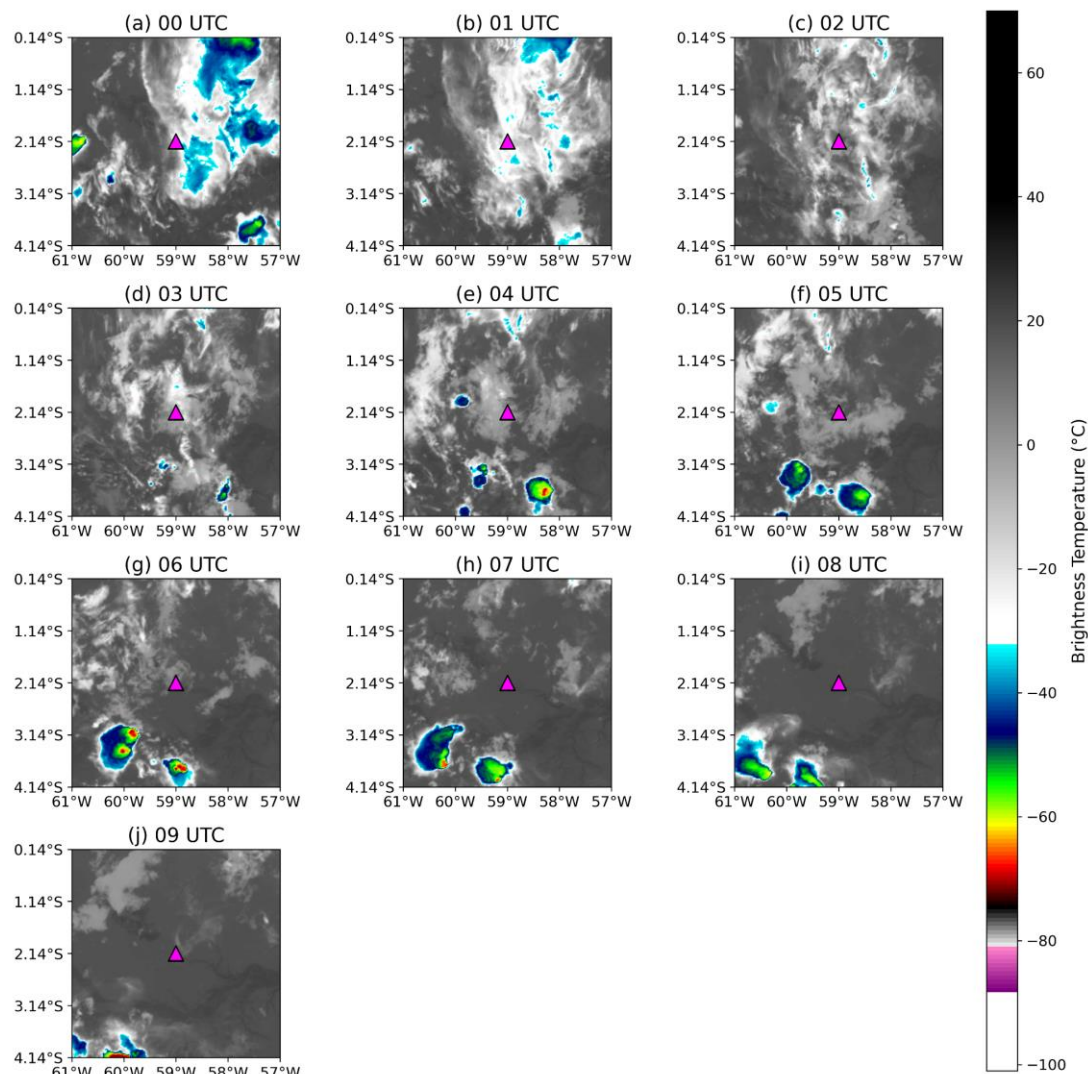
129
 130
 131
 132
 133
 134
 135
 136

Figure 2 (Figure 9 in new version of the manuscript). Nocturnal evolution of (a, b) hourly mean net radiation (Rn) at 81 m (\pm standard deviation), (c, d) cloud fraction (%), (e, f) vertical potential temperature (θ) difference from the value observed at 298 m, and (g, h) vertical wind shear (dU/dz) during the case-study nights of 18 August 2022 (left panels) and 25 August 2022 (right panels). Black horizontal segments indicate the estimated nocturnal boundary layer height at each hour.



137
 138
 139
 140
 141

Figure 3 (Figure S2 in new version of the manuscript). GOES-16 IR Channel 13 (10.3 μm) brightness temperature over the ATTO site on 18 August 2022. Panels (a–j) show hourly images from 00 to 09 UTC. The magenta triangle marks the location of the ATTO tower.



142
 143 Figure 4 (Figure S3 in new version of the manuscript). GOES-16 IR Channel 13 (10.3 μm)
 144 brightness temperature over the ATTO site on 25 August 2022. Panels (a–j) show hourly
 145 images from 00 to 09 UTC. The magenta triangle marks the location of the ATTO tower.

146
 147
 148 We included this new analysis in Section 3.3 of the Results and in the new Discussion section
 149 of the revised manuscript.

150
 151 In section 3.3

152 L239–253: To better identify the main drivers controlling the contrasting hn behavior during
 153 the two case-study nights, we further analyzed R_n at 81m, cloud cover, the vertical profile of
 154 θ and windshear (dU/dz) (Fig. 9). These variables provide complementary information on the
 155 local radiative forcing, cloud modulation of nocturnal cooling, thermal stratification, and
 156 mechanical turbulence generation. The night of 18 August 2022 was characterized by strong
 157 nocturnal radiative cooling (Fig. 9a), reduced cloud occurrence (Fig. 9c and Fig. S2), and a
 158 pronounced vertical potential temperature gradient (Figure 9e). These conditions indicate
 159 enhanced thermal stratification near the surface. Although wind shear was observed at some
 160 levels (Fig. 9g), the strong stratification suggests that mechanically generated turbulence aloft
 161 was not efficiently coupled downward toward the canopy. This supports the interpretation that
 162 the shallow hn observed on 18 August 2022 reflects not only strong thermal stratification, but
 163 also canopy-induced suppression of vertical mixing near the forest top. This configuration is
 164 consistent with a shallow surface-based nocturnal layer that remained partly decoupled from

165 the air above, similar to the layered nocturnal structure described by Mahrt and Acevedo
166 (2023). In contrast, the night of 25 August 2022 showed larger cloud cover (Fig. 9d and
167 Fig.S3), weaker radiative cooling during the early part of the night (Fig. 9b), and weaker
168 thermal stratification (Fig. 9f). Wind shear extended to higher levels (Fig. 9h), reaching
169 approximately 150–170 m, close to the observed hn. This suggests that, under weaker
170 stratification, mechanically generated turbulence was more effectively coupled over a deeper
171 layer, contributing to the larger and more variable hn observed during this night.

172
173 In section 4 - Discussion

174 L289-322: “The results presented here demonstrate that the nocturnal boundary-layer height
175 (hn) above the central Amazon is strongly controlled by the interaction between nocturnal
176 radiative cooling, atmospheric stability, cloud cover, and mechanically generated turbulence.
177 Although previous Amazonian studies have primarily focused on the daytime evolution of the
178 atmospheric boundary layer (Fisch et al., 2004; Carneiro and Fisch, 2020; Dias-Júnior et al.,
179 2022), our results show that the nocturnal boundary layer also exhibits pronounced seasonal
180 and interannual variability, with important implications for turbulence exchange and trace-gas
181 transport above tropical forests.

182
183 One of the clearest patterns observed in this study is the systematic reduction of hn during the
184 Dry season and during the El Niño year (2023). These periods were characterized by stronger
185 nocturnal net radiative loss (Figure 2a) and enhanced atmospheric stability, reflected by larger
186 z/L values (Figure 2b) and a stronger thermal gradient (Fig. S6b, d). Under these conditions,
187 turbulent exchange becomes increasingly suppressed, limiting the upward transport of
188 sensible heat and favoring the formation of shallower nocturnal layers (Figures 4d and 5b). In
189 contrast, wetter conditions, particularly during the Wet season of 2022, were associated with
190 weaker radiative cooling (Figure 2a), reduced stability (Figure 2b), Weak thermal gradient(Fig
191 S6a, c), and deeper nocturnal layers (Figures 4a and 5a). These findings reinforce the strong
192 coupling between cloud cover, nocturnal cooling, and turbulence generation over the Amazon
193 rainforest.

194
195 The hourly evolution of hn also reveals the importance of the temporal evolution of thermal
196 stratification during the night. In all analyzed periods, hn was generally larger at the beginning
197 of the night and progressively decreased toward the early morning hours (Figure 5). This
198 behavior is particularly evident during the Wet season of 2022, when the thermal gradient
199 remained relatively weak during the first hours of the night (Figures 9e,f and S6a), allowing
200 mechanically generated turbulence to sustain a deeper nocturnal boundary layer. As the night
201 progressed, radiative cooling intensified the thermal gradients, suppressing turbulence and
202 leading to a gradual collapse of hn. This progressive reduction of turbulent mixing throughout
203 the night is consistent with the classical evolution of stable nocturnal boundary layers
204 described in previous studies (Mahrt, 1999; Sun et al., 2002).

205
206 The results also demonstrate that the interaction between thermal stratification and
207 mechanically generated turbulence is fundamental for understanding the nocturnal boundary-
208 layer structure above the Amazon forest (Figure 9). The case studies revealed that low-level
209 jets (LLJs) (Figure 7) and enhanced vertical wind shear (Figure 9 g,h) may sustain turbulence
210 above the canopy, but the influence of this turbulence on the lower nocturnal boundary layer
211 depends on the degree of vertical coupling between atmospheric layers. This interpretation is
212 consistent with the conceptual framework proposed by Mahrt and Acevedo (2023), in which
213 nocturnal boundary layers may deviate from a vertically monotonic structure and instead
214 exhibit layered configurations composed of shallow surface-based layers, transition layers,
215 and elevated turbulent regions.

216
217 Our observations suggest that the forest canopy plays a key role in reinforcing this layered
218 structure. Under strongly stable conditions, the canopy acts as a roughness and drag layer
219 that attenuates momentum transfer toward the surface. Consequently, turbulence generated

aloft by LLJs or strong wind shear may remain confined to elevated layers and may not efficiently penetrate downward through the canopy layer. This mechanism likely explains the shallow h_n observed on 18 August 2022, when strong thermal stratification and weak vertical coupling produced a highly decoupled nocturnal structure. In contrast, on 25 August 2022, weaker thermal stratification allowed mechanically generated turbulence to penetrate deeper into the lower nocturnal boundary layer, resulting in larger and more vertically connected h_n values.“

3. In the results, Figure 4, which presents the nocturnal boundary layer height under wet and dry conditions for 2022 and 2023, would benefit from further elaboration. While the results are interesting, the discussion remains largely descriptive. A deeper analysis is needed to explain the origin of the observed differences. In particular, it would be valuable to discuss which physical processes may drive these contrasts and whether they can be linked to other controlling variables. In particular the role of locally driven processes such as stability, turbulence, surface fluxes, or large-scale meteorological conditions, that influence the ANBL.

Our analyses indicate that the seasonal and interannual variability of the ANBL is strongly linked to the modulation of nocturnal radiative forcing by cloud cover. Wetter conditions, associated with increased cloudiness, reduce net longwave radiative loss at the surface, weakening near-surface cooling and limiting the development of strong thermal stratification. In contrast, clearer conditions during the dry season favor stronger radiative loss and a more stable nocturnal boundary layer.

These large-scale meteorological conditions directly influence the efficiency of local turbulent processes controlling h_n . Under weaker stability, turbulence generated by wind shear can more effectively maintain vertical mixing and sustain a deeper nocturnal layer. Conversely, under strongly stable atmospheric conditions, turbulence is suppressed, vertical exchange becomes less efficient, and the ANBL remains shallower.

The case studies analyzed in response to Reviewer Comment (2) support this interpretation by showing that deeper h_n values are associated with weaker stability and enhanced turbulent mixing, whereas shallower h_n occurs during nights characterized by stronger thermal stratification. Based on these results, we interpret the deeper nocturnal layers observed during the wet season of 2022 as a consequence of reduced radiative cooling and weaker stability, while the shallower h_n observed during the dry season of 2023 reflects enhanced radiative cooling and stronger suppression of turbulence. We revised the manuscript to make these physical links clearer in the Results and Discussion sections.

We have added a new discussion addressing this point in the revised version of the manuscript (lines 150–225 of this document).

4. In the same line, and perhaps to support their analysis, perhaps it is interesting to study if there are current formulations (representations) or other methods to estimate the NBL height that are able to reproduce the observational dynamic evolution.

We thank the reviewer for this suggestion. We now added a short discussion of this point in the manuscript.

Several methods can be used to estimate h_n , including criteria based on potential temperature, CO₂, wind speed, Richardson number, and TKE. A recent study at ATTO using field data collected during CloudRoots-Amazon22 (Vila-Guerau de Arellano et al., 2024) observations applied these five criteria and showed that they reproduce the hourly evolution of the nocturnal boundary-layer height, with values ranging from 114 to 241 m and mean estimates between 150 and 188 m (Figure 2 of the Huitema et al., 2026). The same study also

274 showed that h_n was shallower under strongly stable conditions and deeper under weakly
275 stable conditions, consistent with the expected stability-turbulence control.

276

277 In our study, we decided to use the sensible-heat-flux profile method because it is directly
278 linked to the turbulent definition of the nocturnal boundary layer. This choice is also supported
279 by Mendonça et al. (2025, 2026), who showed that vertical profiles of sensible heat flux can
280 be used to estimate h_n at ATTO. Therefore, although other diagnostic methods are available
281 and can reproduce the dynamic evolution of the NBL, we retained the heat-flux-based method
282 because it provides a direct turbulence-based estimate and is consistent with previous ATTO
283 studies.

284

285 We added a new sentence in the manuscript as bellow:

286

287 L344-354: Compared to previous Amazonian studies, the turbulence-based methodology
288 adopted in this work provides an important advantage because it estimates h_n directly from
289 the vertical decay of turbulent sensible heat fluxes. Most previous studies relied on indirect
290 methods based on thermodynamic profiles, Richardson number, or remote sensing
291 approaches (Santos et al., 2007; Dias-Júnior et al., 2022). More recently, Mendonça et al.
292 (2025) used the same turbulence-based methodology and reported h_n values ranging
293 between approximately 81 and 223 m, demonstrating the importance of surface roughness
294 and topography for nocturnal boundary-layer structure. However, their study did not focus on
295 the hourly evolution of h_n or on its relationship with trace-gas concentration profiles. In
296 addition, Huitema et al. (2026), using CloudRoots-Amazon22 observations (Vila-Guerau de
297 Arellano et al., 2024), showed that multiple criteria based on potential temperature, CO₂, wind
298 speed, Richardson number, and turbulent kinetic energy reproduce similar nocturnal
299 boundary-layer dynamics, with estimated values between 114 and 241 m. The agreement
300 between these independent approaches and the results presented here supports the
301 robustness of the observed dynamic evolution of h_n at the ATTO site.

302

303 5. In section 3.3 the role of the canopy deserves more explicit attention. Given the
304 observational setup, the authors are in a unique position to assess how the forest canopy
305 influences the structure and dynamics of the nocturnal boundary layer (see for instance line
306 179 and 225). Although the results (line 223-228) conclude that the canopy plays a role, this
307 influence is not sufficiently specified or supported by analysis. A more detailed discussion,
308 ideally supported by quantitative evidence, of the mechanisms through which the canopy
309 affects nocturnal stratification, turbulence, or mixing would substantially strengthen the
310 manuscript.

311

312 In the revised manuscript, we expanded Section 3.3 to better describe the physical
313 mechanisms through which the Amazon forest canopy influences nocturnal stratification and
314 turbulent mixing. The tall and dense canopy strongly modifies the exchange of momentum
315 and heat enhancing the vertical coupling/decoupling between the surface layer and the
316 atmosphere aloft under stable nighttime conditions.

317

318 Our analysis indicates that during nights with stronger radiative cooling and enhanced thermal
319 stability, turbulence generated above the canopy was not efficiently transported downward
320 through the canopy layer. Under these conditions, the canopy acts as a barrier to vertical
321 mixing, favoring the formation of a shallow and strongly stratified nocturnal layer close to the
322 forest top. This behavior was particularly evident on 18 August 2022, when strong thermal
323 stratification and weak cloud cover were associated with shallow h_n values around 80–100 m.
324 In contrast, during nights with weaker stability and enhanced wind shear, mechanically
325 generated turbulence was able to remain coupled across a deeper layer above the canopy.
326 Under these conditions, the canopy-induced decoupling was weaker, allowing turbulence to
327 extend to higher levels and contributing to deeper and more variable h_n values, as observed
328 on 25 August 2022.

329
330
331
332
333
334
335
336
337
338
339
340
341
342
343
344
345
346
347
348
349
350
351
352
353
354
355
356
357
358
359
360
361
362
363
364
365
366
367
368
369
370
371
372
373
374
375
376
377
378
379
380
381
382
383

To support this interpretation, we added new analyses of vertical profile of the potential temperature gradients, wind shear, cloud fraction, and radiative forcing (Figure 2). These additional results provide quantitative evidence that the canopy influence on hn emerges from its interaction with thermal stratification and mechanical turbulence generation, rather than from a purely local surface effect.

We added a new sentence in the revised version of the manuscript:

L316-323: "Our observations suggest that the forest canopy plays a key role in reinforcing this layered structure. Under strongly stable conditions, the canopy acts as a roughness and drag layer that attenuates momentum transfer toward the surface. Consequently, turbulence generated aloft by LLJs or strong wind shear may remain confined to elevated layers and may not efficiently penetrate downward through the canopy layer."

6. Finally, additional background information would strengthen the results in Figure 8, which compared to two stability cases. More emphasis should be placed on the different background concentrations during the past days of the gases and their effect on the current nocturnal gas exchange. In addition, to truly understand the effect of stability on trace gas concentrations, it would be valuable to compare two nights with similar wind and background trace gas conditions. Especially, because previous papers highlight the complicated CH₄ signal at ATTO with winds from the South-East (Botia et al., 2020).

We agree with the reviewer that it would be valuable to compare nights with similar wind and background trace gas conditions. However, due to the large natural variation of CO and CH₄ concentrations, this is challenging. In the previous version of the manuscript, we included a multi-day figure showing the CO and CH₄ concentrations before and during each case study (Figure S4) which indeed shows that the starting background conditions were not the same for the two case studies.

To improve this part of the manuscript, we first of all have expanded this aspect in the discussion of the revised manuscript. In the text, we now better acknowledge the complexity of CH₄ and CO signals at ATTO as also highlighted by Botía et al. (2020). In addition, in the revised manuscript, we suggest to focus more on vertical gas concentration patterns (differences between upper and lower layers), rather than absolute concentration values. Lastly, we added two additional case studies to the supplement, namely the nights of 02 September 2022 and 28 August 2022.

The case studies were selected to provide an additional comparison of nights with different stability and hn behavior. On 02 September 2022, the nocturnal boundary layer remained shallow, mostly around 80-100 m, and the potential temperature gradient was stronger, reaching values close to -4 K near the canopy (Figure 6a). In this case study, the upper levels (273 and 321m) consistently showed an independent behaviour in comparison to the lower levels (Figure 5a and 5c), indicating that the shallow and stable layer acted as a barrier to vertical exchange (Figure 6).

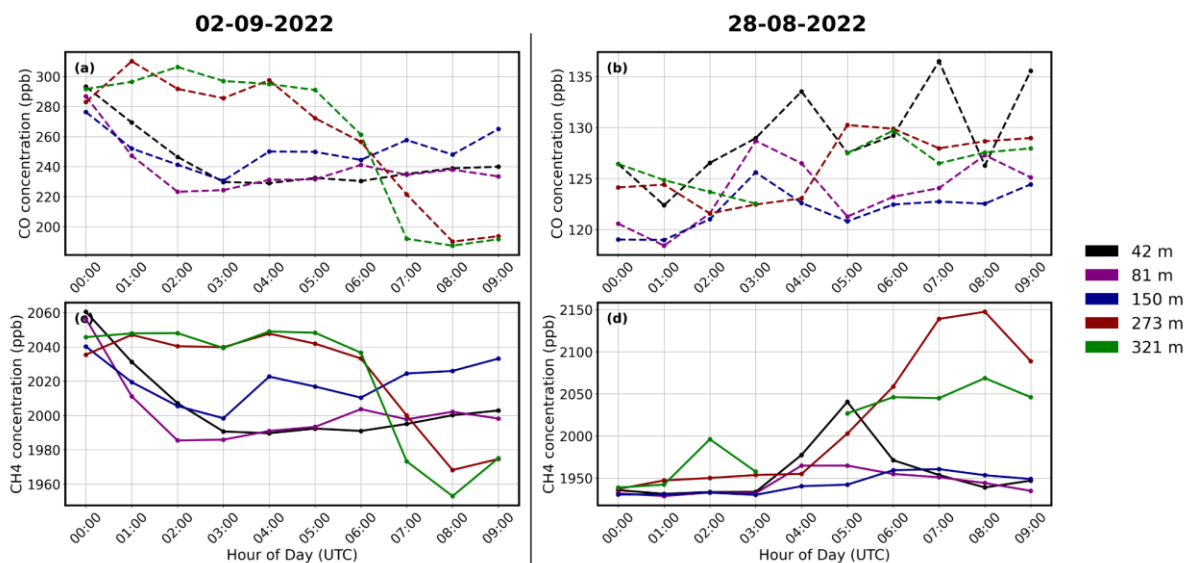
In contrast, on 28 August 2022, the potential temperature gradient was weaker, approximately -2 K (Figure 6b) near the canopy top, hn was deeper and more variable, and decreasing during the night. This temporal behaviour is visible also in the gas concentrations, especially for CH₄, where at 5:00 the hn separated the upper levels from the lower levels, after which the upper levels started to behave differently, and demonstrating the possible arrival of a new enriched air mass (Figure 7).

These two additional cases also exemplify the interaction between the hn and the initial or background concentrations prior to the evolution of the nocturnal event. In the first one

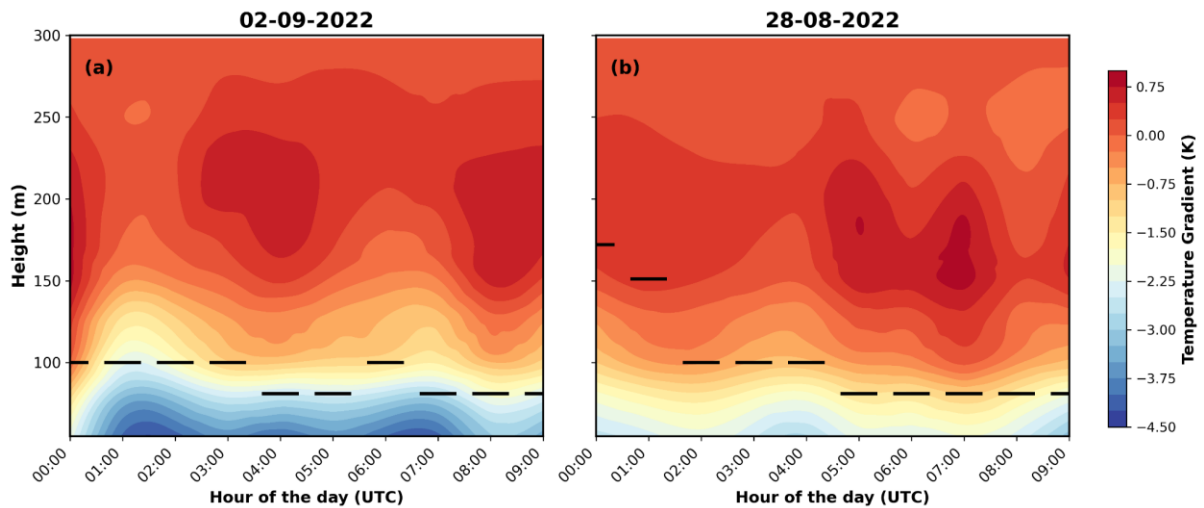
384 (02.09.2022) the initial concentrations are relatively high, since previous hours, at all levels
 385 (~290 ppb CO and ~2050 for CH₄) compared to the rest of the night. The weak decoupling
 386 (~40 ppb in both CH₄ and CO) between 273-321 m and the levels below, is due to the shallow
 387 hn (80-100 m) which disconnects the layers closer to the canopy, with low CH₄ and CO, and
 388 leading to a dilution of the initial mole fractions at the levels below 273 m. In contrast, the trace
 389 gases at 273-321 m remain with small variability relative to their initial state because the
 390 measurement height is above the hn.

391
 392 In the new version of the manuscript we added the following sentence:
 393

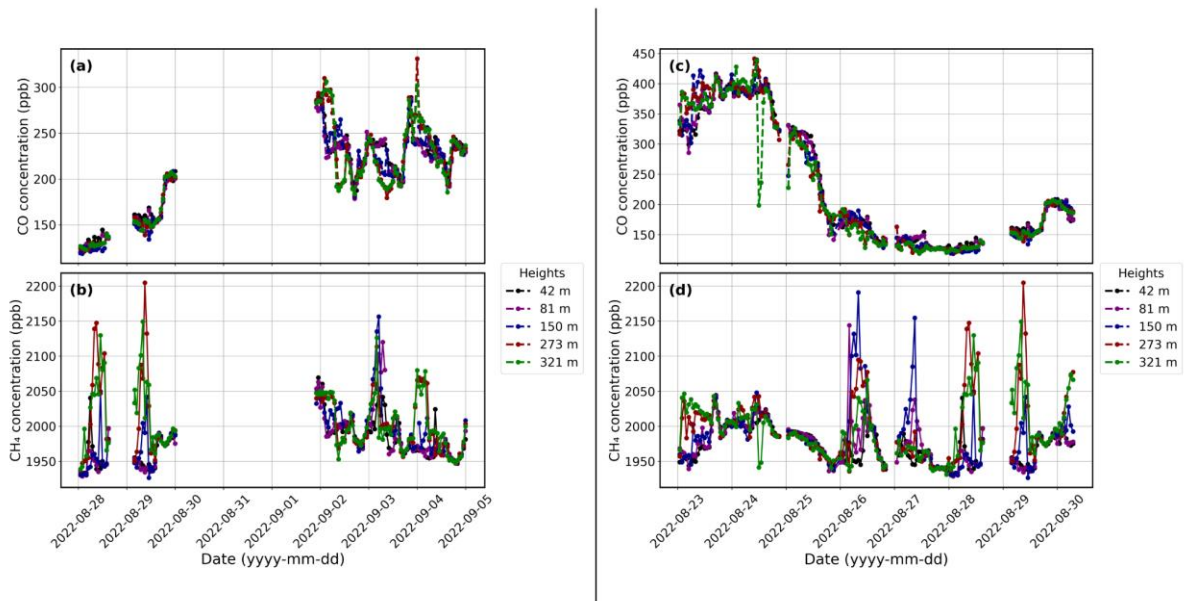
394 L328-343: The interpretation of these concentration patterns must also consider the
 395 background atmospheric composition during previous days. As discussed by Botía et al.
 396 (2020), the ATTO site frequently experiences nighttime CH₄ accumulation associated with
 397 strong thermal stratification, suppressed turbulence, and horizontal transport from likely
 398 wetland source regions. In addition, CO concentrations are strongly influenced by regional
 399 biomass-burning plumes (Andreae et al., 2015; Van Asperen et al., 2024). For example, the
 400 elevated CO and CH₄ concentrations observed on 25 August 2022 likely reflected the residual
 401 influence of previous plume events (Figure S5) combined with slower ventilation near the
 402 canopy. Therefore, rather than associating multi-day concentration variability directly with hn,
 403 our interpretation focuses on the short-term vertical concentration gradients and their
 404 relationship with nocturnal turbulent structure. The additional case studies presented in the
 405 Supplement further reinforce this interpretation (Fig. S7). Strongly stable nights with shallow
 406 hn (Fig. S8a) exhibited clear vertical separation between upper and lower layers (Fig. S7a,c),
 407 while less stable nights with deeper hn (Fig S8b) showed much more homogeneous
 408 concentration patterns throughout the tower profile (Fig. S7b, d). The supplementary cases
 409 also show the importance of the initial/background concentrations from the previous days in
 410 shaping the nocturnal CO and CH₄ profiles (Fig. S9). As in the 18 and 25 August cases, the
 411 vertical gradients were influenced not only by the evolution of hn, but also by the concentration
 412 structure already present before the night. These consistent relationships between hn and the
 413 observed concentration gradients provide independent observational support for the
 414 turbulence-based estimates of nocturnal boundary-layer height presented here.
 415
 416



417
 418 Figure 5 (Figure S7 in the new version of the manuscript). Hourly mean vertical profiles of CO
 419 and CH₄ concentrations during two additional nocturnal case studies: 02 September 2022,
 420 while panels (c) and (d) show CO and CH₄, respectively, for 28 August 2022
 421
 422



423
 424 Figure 6 (Figure S8 in the new version of the manuscript). Time-height evolution of the vertical
 425 potential temperature gradient during the nights of 02 September 2022 and 28 August 2022.
 426 Panels (a) and (b) show the respective nights, with dashed black lines indicating the estimated
 427 nocturnal boundary-layer height h_n
 428



429
 430 Figure 7 (Figure S9 in the new version of the manuscript). Multi-day evolution of CO and CH₄
 431 concentrations at different sampling heights before and during the selected nocturnal case
 432 studies. Panels (a) and (b) show CO and CH₄, respectively, for the period including 02
 433 September 2022, while panels (c) and (d) show CO and CH₄, respectively, for the period
 434 including 28 August 2022.
 435
 436

437 References:

438
 439 Botía, S., Gerbig, C., Marshall, J., Lavric, J. V., Walter, D., Pöhlker, C., ... & Acevedo, O. C. (2020).
 440 Understanding nighttime methane signals at the Amazon Tall Tower Observatory (ATTO). *Atmospheric*
 441 *Chemistry and Physics*, 20(11), 6583-6606.
 442
 443 Mendonça, A., Dias, C. Q., Acevedo, O. C., Marra, D. M., Cely-Toro, I. M., Fisch, G., ... & Mortarini, L.
 444 (2025, January). Nocturnal Boundary Layer Height Estimated from Direct Turbulence Measurements at
 445 the ATTO Tower. In *105th Annual AMS Meeting 2025* (Vol. 105, p. 446515).
 446

447 Mendonça, A. C., Dias-Junior, C. Q., de Oliveira, M. I., Maroneze, R., Martins, L. G. N., Marra, D. M.,
448 ... & Acevedo, O. C. (2026). Is Low-Level Jet height a good approximation for the top of the nocturnal
449 boundary-layer?. *Agricultural and Forest Meteorology*, 380, 111065.
450
451 Huitema, A. C., de Feiter, V. S., González-Armas, R., Hartogensis, O. K., van Asperen, H., Quaresma
452 Dias-Júnior, C., & Vilà-Guerau de Arellano, J. (2026). CO 2 and Heat exchange across the Nocturnal
453 Canopy–Atmosphere interface in the Amazon rainforest. *EGUsphere*, 2026, 1-32.
454
455 Mahrt, L., & Acevedo, O. (2023). Types of vertical structure of the nocturnal boundary layer. *Boundary-*
456 *Layer Meteorology*, 187(1), 141-161.
457
458 Souza Jr, C. M., Marengo, J., Ferreira, B., Ribeiro, J., Schirmbeck, L. W., Schirmbeck, J., ... & Latuf, M.
459 O. (2024). Amazon severe drought in 2023 triggered surface water loss. *Environmental Research:*
460 *Climate*, 3(4), 041002.
461
462 Vila-Guerau de Arellano, J., Hartogensis, O. K., De Boer, H., Moonen, R., González-Armas, R.,
463 Janssens, M., ... & Röckmann, T. (2024). CloudRoots-Amazon22: Integrating clouds with
464 photosynthesis by crossing scales. *Bulletin of the American Meteorological Society*, 105(7), E1275-
465 E1302.